

Crack Propagation in Ceramic Materials Under Cyclic Loading Conditions

A. G. EVANS AND E. R. FULLER

An analysis is presented which enables crack propagation rates under cyclic loading conditions to be predicted from static slow crack growth parameters. A comparison of the predicted times to failure under cyclic conditions with available measured failure times, for several ceramic materials at ambient temperatures, suggests that there is no significant enhancement of the slow crack growth rate due to cycling. This is verified in a series of measurements of slow crack growth rates under static and cyclic conditions.

FOR static loading of metallic materials, slow crack growth can occur, for example, due to stress corrosion¹ and hydrogen embrittlement.² For these processes, the crack velocity (da/dt) during crack propagation depends primarily on the stress intensity factor, K_I , and it is frequently observed that,³

$$\left(\frac{da}{dt}\right) = AK_I^n, \quad [1]$$

where A and n are system constants which depend only on the environment and the temperature. When cyclic loading is imposed, an independent source of slow crack growth can function. This mode of crack propagation depends primarily on the amplitude of the cycle, ΔK_I , such that the crack growth per cycle, da/dN , is frequently given for a limited range of ΔK_I by,^{4,5,6,7}

$$\left(\frac{da}{dN}\right) = B(\Delta K_I)^{n^*} \quad [2]$$

where B and n^* are system constants.

In ceramic materials, the existence of static (environmentally dependent) slow crack growth is now well established.^{8,9} The rate of crack propagation in the region of practical interest is determined exclusively by the stress intensity factor, K_I , as it is for metallic materials (Eq. [1]). Slow crack growth under cyclic loading conditions is also observed,^{10,11,12} But, it has frequently been suggested that there is no enhanced effect of cycling on the crack propagation rate. It is intended in this paper to develop relations which predict the crack growth rate (or time to failure) under cyclic loading conditions from the static slow crack growth parameters. This can then be compared with experimental measurements of crack growth rate under cyclic conditions to establish whether there is an enhanced effect on the crack growth rate due to cycling.

The only available experimental measurements under cyclic loading are time-to-failure measurements, Refs. 10 to 12. These are subject to considerable statistical variation and it is difficult to obtain effective comparisons with static measurements. A technique for obtaining more precise comparisons is thus developed. It is based on crack velocity measurements for both static and cyclic loading situations. Finally,

crack velocity data are obtained for two ceramic materials using this technique, and the measured variations are compared with those predicted analytically.

I. CRACK GROWTH RATE UNDER CYCLIC CONDITIONS

In this section, the crack growth rate expected under cyclic loading is evaluated for the condition that the growth rate is exclusively dependent on the static slow crack growth parameters. Applying the general condition,

$$K_I = Y\sigma a^{1/2} \quad [3]$$

where σ is the applied stress and Y is a geometrical factor, and substituting for K_I in Eq. [1] gives,

$$a^{-n/2} \frac{da}{dt} = AY^n \sigma^n. \quad [4]$$

Integrating Eq. [4] to obtain the crack growth in time, t , gives,

$$\begin{aligned} & [2/(n-2)AY^n] \left[(1/a_i)^{(n-2)/2} - (1/a)^{(n-2)/2} \right] \\ & = \int_0^t [\sigma(t')]^n dt', \end{aligned} \quad [5]$$

where the initial crack length a_i is related to the initial stress intensity factor K_{Ii} and initial stress σ_i through Eq. [3]. The time to failure may be obtained from Eq. [5] and is given by the time for a crack to propagate from an initial subcritical size, a_i , to a critical size, a_c , determined by the condition that $K_I = K_{IC}$, the critical stress intensity factor.

For static loading, $\sigma(t) = \sigma_s$, and the time to failure, t_s , is given directly from Eqs. [3] and [5] as

$$t_s = [2/(n-2)AY^2\sigma_s^2 K_{IS}^{n-2}] [1 - (K_{IS}/K_{IC})^{n-2}], \quad [6]$$

where $K_{IS} = Y\sigma_s a_i^{1/2}$. For ceramic materials, n is typically a large number¹³ (9 to 60). Thus, $(K_{IS}/K_{IC})^{n-2} \ll 1$ (except for short times to failure) and to a good approximation¹³

$$t_s \cong [2/(n-2)AY^2\sigma_s^2 K_{IS}^{n-2}]. \quad [7]$$

For cyclic loading, the stress is periodic with an average value, σ_a , amplitude, $\sigma_0 (= \zeta\sigma_a)$, and frequency $\omega = 2\pi/\lambda$, where λ is the period. If the time to failure for cyclic loading, t_c , is expressed as an integer number

A. G. EVANS and E. R. FULLER, are Project Leader and Postdoctoral Fellow, respectively, Inorganic Materials Division, National Bureau of Standards, Washington, D.C. 20234.

Manuscript submitted April 30, 1973.

of cycles $N\lambda$ plus a fraction of a cycle $\delta\lambda$, the integral on the right-hand side of Eq. [5] can be written as

$$\int_0^{t_c=(N+\delta)\lambda} [\sigma(t)]^n dt = \sigma_a^n g(n, \zeta) t_c \cdot \left[\left(N + \frac{\int_0^{\delta\lambda} \sigma^n dt}{\int_0^\lambda \sigma^n dt} \right) / (N + \delta) \right] \approx \sigma_a^n g(n, \zeta) t_c \quad (\text{for } N \gg 1), \quad [8]$$

where

$$g(n, \zeta) = \frac{1}{\lambda} \int_0^\lambda [\sigma(t)/\sigma_a]^n dt. \quad [9]$$

The left-hand side of Eq. [5] can be related to the static loading result, Eq. [6]; and the ratio of the cyclic time to failure to the static time to failure for an initial flaw of length a_i is

$$t_c/t_s = g^{-1}(\sigma_s/\sigma_a)^n \frac{\left[1 - \left(\frac{K_{II}}{K_{IC}} \right)^{n-2} \left(\frac{\sigma_f}{\sigma_i} \right)^{n-2} \right]}{\left[1 - \left(\frac{K_{IS}}{K_{IC}} \right)^{n-2} \right]} \frac{[1 + \delta/N]}{\left[1 + \frac{1}{N\lambda g} \int_0^{\delta\lambda} [\sigma/\sigma_a]^n dt \right]} \quad [10]$$

where σ_i and σ_f are the initial and final stresses and $K_{II} = Y\sigma_i a_i^{1/2} = (\sigma_i/\sigma_s)K_{IS}$. For a large number of cycles to failure, $N \gg 1$,* the difference between t_c and

*This corresponds to the condition, $\zeta \leq [(K_{IC} - K_{II})/(K_{IC} + K_{II})]$.

$N\lambda$ is negligible, and Eq. [10] can be written to a good approximation as

$$t_c/t_s \approx g^{-1}(\sigma_s/\sigma_a)^n. \quad [11]$$

Thus, if there is no enhanced cyclic effect on the crack growth rate, the time to failure is amplitude dependent through the factor g^{-1} ,* and frequency independent.

*Pseudo-amplitude dependence may occur from the ratio $[\sigma_s/\sigma_a]^n$, if for example, $\sigma_s = \sigma_a + \sigma_o = \sigma_a [1 + \zeta]$. But here the effect of increasing the amplitude at constant static load is equivalent to decreasing the average cyclic load.

1) The Evaluation of g

A case of particular practical importance is the sinusoidal stress,

$$\sigma(t) = \sigma_a + \sigma_o \sin \omega t \quad [12]$$

An analytical solution for g cannot be obtained for this case, but a series solution is possible when n is integer. First, expand $[\sigma/\sigma_a]^n = [1 + \zeta \sin \omega t]^n$ in a binomial series,

$$[\sigma/\sigma_a]^n = \sum_{k=0}^n \binom{n}{k} \zeta^k \sin^k \omega t. \quad [13]$$

Writing $\sin \omega t = (1/2i)(e^{i\omega t} - e^{-i\omega t})$ and expanding $\sin^k \omega t$ as a binomial series Eq. [13] becomes

$$[\sigma/\sigma_a]^n = \sum_{k=0}^n \sum_{l=0}^k \binom{n}{k} \binom{k}{l} (\zeta/2i)^k (-1)^l e^{i(k-2l)\omega t} \quad [14]$$

The average of $e^{i[k-2l]\omega t}$ over one period vanishes, unless $k = 2l$, so that

$$g = \sum_{l=0}^n \sum_{k=2l}^n \binom{n}{k} \binom{k}{l} (\zeta/2i)^k (-1)^l \delta_{k,2l} \quad [15]$$

where the summations over k and l have been interchanged, and $\delta_{k,2l}$ is the Kronecker delta. Since k varies from l to n , and $k = 2l$, the summation over l can only give nonzero values for $l \leq n/2$. Thus,

$$g(n, \zeta) = \sum_{l=0}^{[n/2]_T} \left[\frac{n!}{(n-2l)!(l!)^2} \right] (\zeta/2)^{2l}, \quad [16]$$

where $[n/2]_T$ is the truncated value of $n/2$. Solutions for g can be obtained quite simply from Eq. [16] for various n and ζ . A plot of g^{-1} vs the relative amplitude, ζ , is shown in Fig. 1 for selected values of n .

The lower and upper bounds of g^{-1} for the sinusoidal stress are respectively the g^{-1} for a square wave stress and a saw-tooth stress. These are special cases of the trapezoidal stress solution (given in Appendix A). The results for the square wave stress are

$$g(n, \zeta) = \frac{1}{2} [(1 + \zeta)^n + (1 - \zeta)^n] = \sum_{l=0}^{[n/2]_T} \left[\frac{n!}{(n-2l)!(2l)!} \right] \zeta^{2l}, \quad [17]$$

and for the saw-tooth stress wave

$$g(n, \zeta) = \frac{1}{2(n+1)\zeta} [(1 + \zeta)^{n+1} - (1 - \zeta)^{n+1}] = \sum_{l=0}^{[n/2]_T} \left[\frac{n!}{(n-2l)!(2l+1)!} \right] \zeta^{2l}. \quad [18]$$

These functions are plotted in Figs. 2 and 3, respectively, and the series expansion is given for comparison with the sine wave result.

Finally, it should be mentioned that the relative amplitude ζ is restricted to the range $0 \leq \zeta \leq 1$. For relative amplitudes greater than one, the stress goes through a compression region, during part of its cycle, where no crack growth can occur. This portion of the cycle must accordingly be omitted when calculating g . Since tension/compression cycles are frequently used in practice, the case of a sinusoidal stress wave about a zero average stress is considered in Appendix B.

II. COMPARISON WITH AVAILABLE TIME-TO-FAILURE MEASUREMENTS

There are few measurements of time to failure under cyclic loading conditions which can be compared directly with measurements made under static loading conditions. The most recent data, which are also the most comprehensive, have been obtained for polycrystalline alumina by Krohn and Hasselman.¹⁰ Using a statistical plotting technique,¹³ we first obtain n for the system from the static data (Fig. 4(a)). This gives 50 ± 5 as the best value. Using this n and taking g from Fig. 1, the failure times under cyclic loading conditions can be predicted from the static data. These predictions are compared with experimental measurements, for three relative amplitudes, in Fig. 4(b). Most of the cyclic data lie within the range of failure times predicted from the static data, although the wide variability makes precise comparison difficult. We can only conclude at this stage, therefore, that the failure of polycrystalline alumina subjected to cyclic loads (superimposed on a constant average tensile load) is due

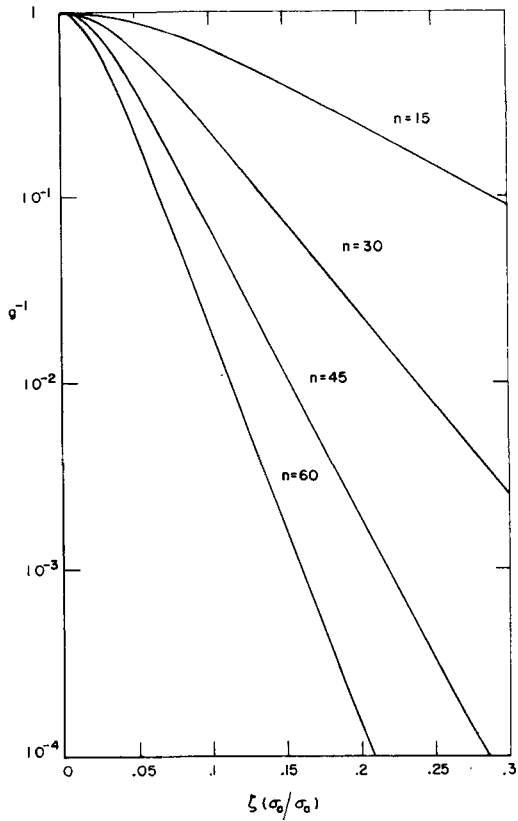


Fig. 1—The time-to-failure ratio, g , for a sinusoidal wave form as a function of the stress amplitude-average stress ratio, ζ , for selected n .

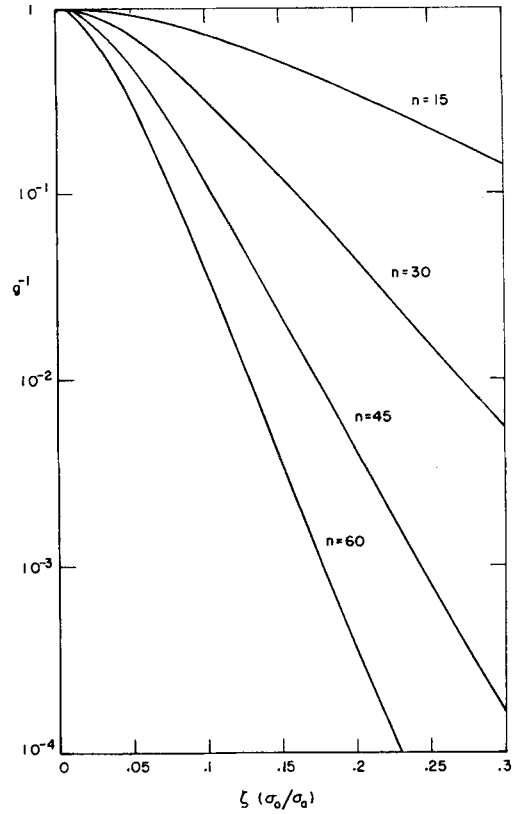


Fig. 3—The time-to-failure ratio, g , for a saw-tooth wave form.

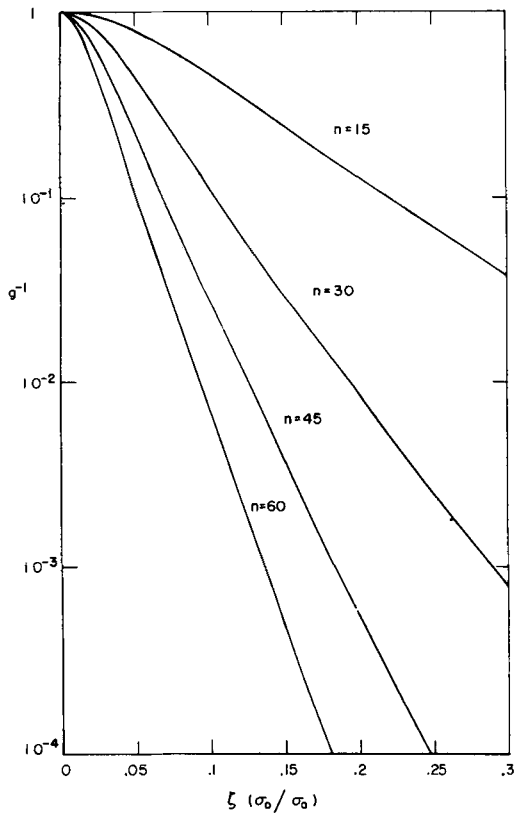


Fig. 2—The time-to-failure ratio, g , for a square wave form.

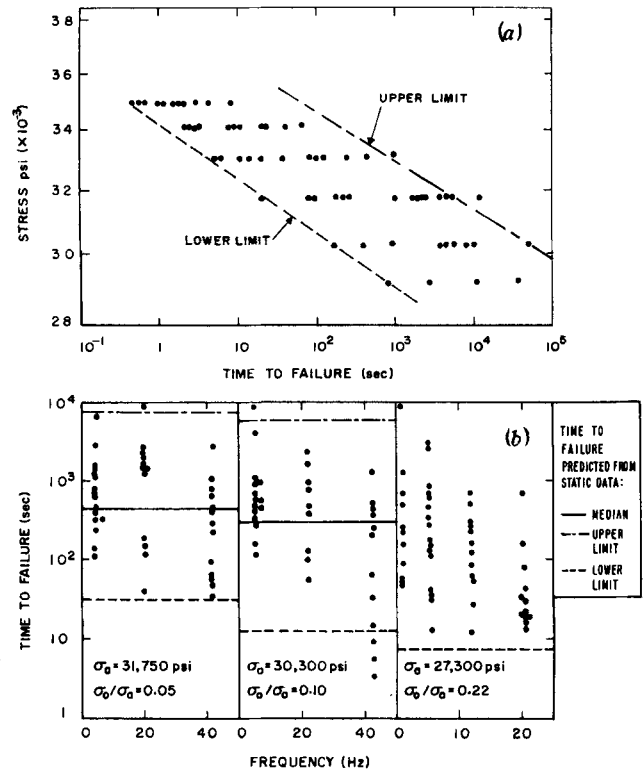


Fig. 4—(a) Static time-to-failure data for polycrystalline alumina (after Krohn and Hasselman). (b) A comparison of cyclic time-to-failure data measured on the same alumina with the time to failure predicted from the static data, using g from Fig. 1.

largely to the conventional stress corrosion process, and that a smaller effect due to cycling may exist, particularly at high frequencies* (≥ 40 Hz).

*This is an ambiguous point because an additional problem associated with making cyclic time-to-failure comparisons at different frequencies (as in Fig. 4b) concerns the large effect of the shape of the wave form on g (see Figs. 1, 2, 3). The wave forms must be *identical* if effective time-to-failure comparisons are to be made, and this is difficult to achieve in practice.

The other available cyclic data is for glass¹² and alumina.¹¹ The data for both materials show that the time to failure under cyclic loading is less than the time to failure under static loading at the equivalent *maximum* stress. Yet the analysis (Appendix B) would predict that the time to failure for cyclic loading under these conditions should be *larger* than that for static loading if the slow crack growth is due exclusively to stress corrosion. There is, however, an anomaly associated with these comparisons. The static measurements are made in bending (of rods), whereas the cyclic measurements are made in a rotating/bend fixture, which exposes a much larger surface area to the maximum tensile stress. The fast fracture strength in the rotating/bending mode (σ_{rb}) is thus expected to be lower than in the bending mode (σ_b), due to the statistically related volume dependence of strength.¹⁴ This strength ratio is given by,¹⁴ $\sigma_{rb}/\sigma_b \approx (\theta/2\pi)^{1/m}$, where m is a measure of the strength distribution¹⁵ in the glass or alumina and θ is the included angle, at the maximum tensile stress, in the bend experiment. The ratio of failure times (τ) in the two modes at constant applied stress is thus,¹³ $\tau_{rb}/\tau_b \approx (\theta/2\pi)^{n/m}$. For both glass and alumina, n is almost invariably larger than m (see for example Ref. [13]), and it can reasonably be expected that $\theta/2\pi \leq 1/10$. The effect will therefore be very large and will more than counteract the increase due to g in Eq. [B1].

It may be concluded from available cyclic time-to-failure data, therefore, that the existence of an enhanced effect of cycling on the slow crack growth rate has not been established.

III. STATIC/CYCLIC COMPARISONS FROM CRACK VELOCITY MEASUREMENTS

3.1 The Double Torsion Technique

The problems associated with making precise static/cyclic comparisons from time-to-failure measurements suggest that an improved method for comparison should be devised. The requisite improvement can be achieved by comparing crack growth rates for the two loading conditions, because the constraint due to flaw size variations is essentially removed. A convenient method for measuring crack growth rates in ceramic materials entails the use of a double torsion specimen under constant displacement conditions.^{9,16} This gives the crack velocity for static conditions from the rate of load relaxation;⁹

$$\frac{da}{dt} = -\frac{a_i P_i}{P^2} \left(\frac{dP}{dt} \right)_y, \quad [19]$$

where P is the load, a_i and P_i are the initial values of the crack length and load respectively, and y is the displacement. The corresponding stress intensity factor is then obtained from,^{16,17}

$$K_I = PW_m \left[\frac{3(1+\nu)}{Wd^3d_n} \right]^{1/2} \equiv \beta P \quad [20]$$

where W , W_m , d , and d_n are specimen dimensions (see Ref. 16) and ν is Poisson's ratio. Similarly, for cyclic loading, it can easily be shown that the increment in crack length during one cycle, δa , is given by

$$\delta a = -\frac{a_i P_i (\delta P)}{P(P + \delta P)}, \quad [21]$$

where δP is the load decrement during a cycle measured between points of constant displacement y .

The double torsion specimen can thus be used to obtain both the $K_I - da/dt$ curve for static loading and relationships between the average velocity per cycle, the stress intensity factor and the stress intensity amplitude, ΔK_I , for cyclic loading. It is also possible with this technique to make direct static/cyclic comparisons on a single specimen so that the microstructural variability constraint is minimized.

3.2 Comparison of Static and Cyclic Behavior—Analytical

The comparison of static and cyclic slow crack growth from crack velocity measurements requires analytical values for the average velocity per cycle calculated in terms of the static slow crack growth parameters.

For the double torsion specimen,^{9,16,17}

$$y = P(\alpha a + \gamma) \quad [22]$$

where α is a constant and γ is a constant ≈ 0 for ceramic materials. Substituting the static slow crack growth parameter from Eq. [1] and eliminating P give

$$y^n dt = \frac{1}{A} \left(\frac{\alpha}{\beta} \right)^n a^n da \quad [23]$$

Integration for a periodic displacement with a constant average, y_a , and amplitude, y_0 ($= \xi y_a$), gives

$$\int_0^t [y(t')/y_a]^n dt' = \frac{1}{(n+1)Ay_a^n} \left(\frac{\alpha}{\beta} \right)^n [a^{n+1} - a_i^{n+1}] \quad [24]$$

The left-hand integral is $g\lambda$, as evaluated in section I. For one cycle, therefore,

$$g = \frac{1}{(n+1)Ay_a^n} \left(\frac{\alpha}{\beta} \right)^n \frac{a_i^{n+1}}{\lambda} \left[\left(\frac{a_i + \delta a}{a_i} \right)^{n+1} - 1 \right] \quad [25]$$

If the crack length increment per cycle is small this reduces to

$$g = \left(\frac{\alpha}{\beta} \right)^n \frac{\delta a}{A\lambda} \left(\frac{a_i}{y_a} \right)^n. \quad [26]$$

From Eqs. [20] and [22]

$$y_a = \left(\frac{\alpha}{\beta} \right) K_{Ia} a_i \quad [27]$$

where K_{Ia} is the average stress intensity factor for a cycle. Substituting for y_a in Eq. [26] gives the average crack velocity per cycle.

$$\frac{\delta a}{\lambda} = gAK_{Ia}^n \quad [28]$$

Comparing this with the static solution (Eq. [1]) shows that the ratio of the crack velocities under cyclic and static loading will be given by g (for equivalent K_I) if there is no enhanced effect of cycling on the rate of slow crack growth.

3.3 Comparison of Static and Cyclic Behavior—Experimental

Using double torsion specimens, we compare crack velocities under static and cyclic loading for two ceramic materials—porcelain and glass.* The data ob-

*The glass is a soda-lime glass and the porcelain is an electrical porcelain containing quartz particles $\sim 20 \mu\text{m}$ in diam.

tained are plotted in Figs. 5 and 6. The cyclic experiments were conducted on an Instron testing machine, so the shape of the deflection cycle was essentially trapezoidal (see Appendix A). The exact characteristics of the cycle were obtained from an oscilloscope trace and appropriate values for g computed. Using these g values, the crack velocities per cycle can be evaluated from the static velocity data and compared with the measured crack velocities (Figs. 5 and 6). In all cases, there is no significant difference between the measured crack velocities and the velocities predicted from the static slow crack growth. We conclude, therefore, that for these ceramic materials within the range of frequencies used ($\leq 20 \text{ Hz}$), there is no enhanced effect of cycling on the rate of slow crack growth.

IV. DISCUSSION

It is shown in the preceding sections that the room temperature slow crack growth in several ceramic materials under cyclic loading conditions can be attributed primarily to the static slow crack growth process. The materials analyzed—glass, porcelain, and alumina—do not exhibit significant plastic deformation during crack propagation at room temperature.^{18,19} It would perhaps be anticipated, therefore, that these materials should not show an enhanced effect of cycling on the crack propagation rate, because cyclic fatigue phenomena are generally attributed to defect production due to plastic deformation in the vicinity of the crack tip.²⁰ At higher temperatures, however, where plastic deformation is observed to accompany crack propagation, *e.g.*, above 400°C for alumina,¹⁸ an enhanced effect of cycling may be observed. It is clearly of importance, therefore, to compare static and cyclic slow crack growth at elevated temperatures, and it is intended to make these comparisons using the double torsion technique which can be readily adapted for high temperature use.

For low temperature structural applications of the ceramic materials studied here, the absence of an enhanced effect of cycling results in a very substantial simplification of the failure prediction procedure. It is simply required to obtain relationships between K_I and da/dt for static loading and then to apply the appropriate g to obtain the time to failure. For example, the minimum time to failure τ_{\min} under static load σ_s after proof testing is given by,¹³

$$\tau_{\min} = \frac{2}{(n-2)AY^2\sigma_s^2 K_{IC}^{n-2}} \left(\frac{\sigma_p}{\sigma_s}\right)^{n-2} \quad [29]$$

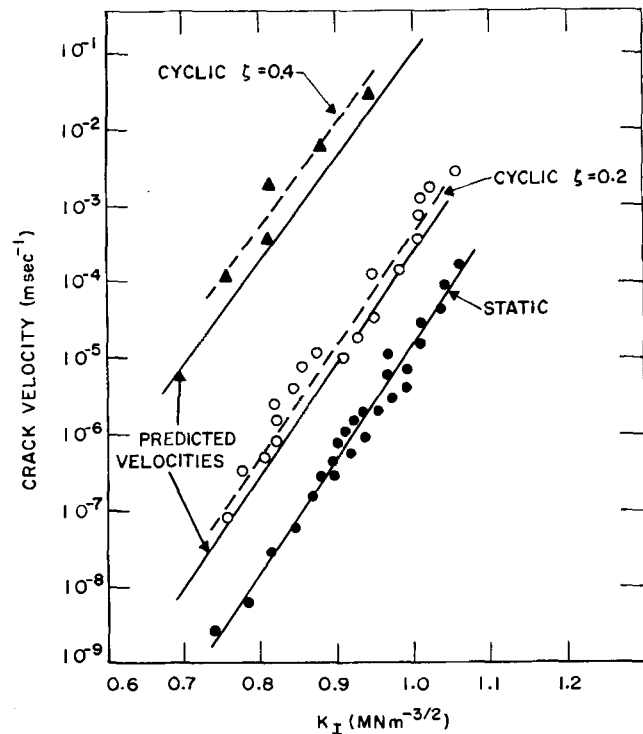


Fig. 5—Crack velocity measurements under static and cyclic loading conditions for porcelain, including cyclic velocities predicted from the static measurements.

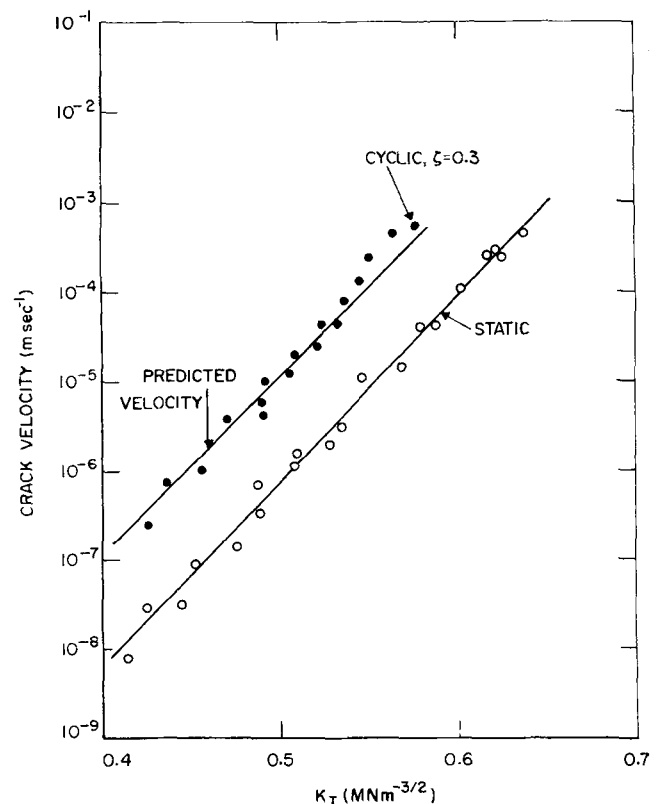


Fig. 6—Static and cyclic crack velocity measurements for glass, showing the cyclic velocities predicted from the static data.

where σ_p is the proof stress. If there is a cyclic component superimposed on the static stress, the minimum time to failure is simply reduced by an amount equivalent to g .

Finally, it is interesting to develop the relationship between crack velocity and stress intensity amplitude from the static slow crack growth parameters and to compare them with the relation obtained for a cyclic fatigue process (Eq. [2]). It will then be possible to specify the distinguishing features of the two slow crack growth processes under cyclic loading. The crack growth per cycle, obtained from the static parameters (Eq. [28]) is

$$\frac{da}{dN} = \lambda g A K_{Ia}^n \quad [30]$$

Using an expansion for g which applies for $\xi \geq 0.1$, the crack growth per cycle for a saw-tooth wave form becomes,

$$\frac{da}{dN} \approx \lambda A K_{Ia}^n \left(\frac{2^n}{n+1} \right) \frac{\exp \left[\frac{(n-1)}{4} \left(\frac{\Delta K_I}{K_{Ia}} \right) \right]}{\exp \left[\frac{(n-1)}{2} \right]} \quad [31]$$

It is apparent from Eq. [31] that (da/dN) depends on both K_I and ΔK_I , and upon the frequency $(1/\lambda)$. Whereas for conventional cyclic fatigue, (da/dN) is dependent primarily on the amplitude, ΔK_I , independent of the frequency.

V. CONCLUSION

An analysis is presented which predicts the slow crack growth under cyclic conditions from the static slow crack growth parameters. A comparison of available time-to-failure measurements made for glass and alumina under static and cyclic conditions with the predicted effects does not give any precise information due to the wide experimental variation of failure times and/or the incompatibility of the static and cyclic measurements.

A comparison of crack growth rates for static and cyclic loading, using the double torsion technique, for two ceramic materials—glass and porcelain—shows that the cyclic crack growth rates are due primarily to the static slow crack growth mechanism. There is no significantly enhanced effect of cycling. The simple approach to failure prediction that can be used with materials that do not exhibit an enhanced cycling effect is outlined.

APPENDIX A

g FACTOR FOR A TRAPEZOID STRESS WAVE

In this appendix the g factor relating the time to failure, t_c , for a trapezoid stress wave to the time to failure, t_s , for a static stress, $\sigma_s (= \sigma_a)$ is evaluated. The wave form is illustrated in Fig. 7. It should be noted that the h 's must sum to one, $\sum_{i=1}^8 h_i = 1$, and that σ_a is no longer the average stress unless $h_1 + h_3 + 2h_2 = h_5 + h_7 + 2h_6$. The integral, Eq. [9], is easily performed by splitting it into eight parts. The result is

$$t_s/t_c = g(n, \xi) = (h_4 + h_8) + [h_2(1 + \xi)^n + h_6(1 - \xi)^n] + \frac{1}{(n+1)\xi} \left\{ (h_1 + h_3)[(1 + \xi)^{n+1} - 1] + (h_5 + h_7)[1 - (1 - \xi)^{n+1}] \right\} \quad [A1]$$

There are several interesting special cases of this

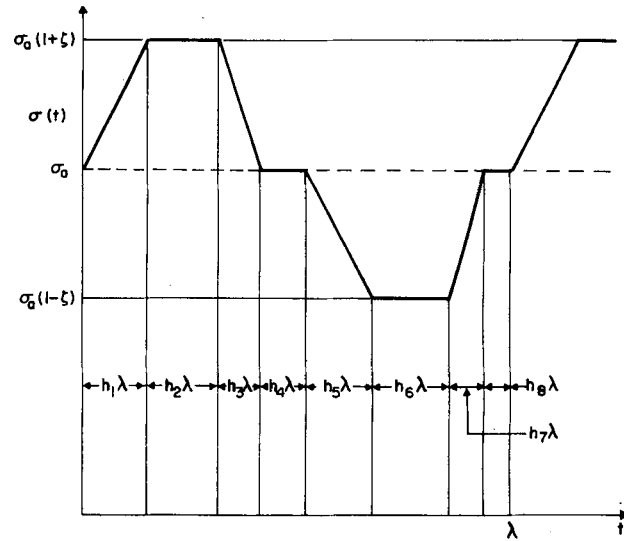


Fig. 7—A schematic representation of the general trapezoidal cycle used for analysis.

general result. A square wave stress is obtained for $h_1 = h_3 = h_5 = h_7 = h_4 = h_8 = 0$ and $h_2 = h_6 = \frac{1}{2}$ to give

$$g(n, \xi) = \frac{1}{2} [(1 + \xi)^n + (1 - \xi)^n] \quad [A2]$$

A saw-tooth stress wave requires $h_2 = h_4 = h_6 = h_8 = 0$ and $h_1 + h_3 = h_5 + h_7 = \frac{1}{2}$ to give

$$g(n, \xi) = \frac{1}{2(n+1)\xi} [(1 + \xi)^{n+1} - (1 - \xi)^{n+1}] \quad [A3]$$

Note that the result is independent of the way in which the stress peaks and drops over a half period, $\lambda/2$.

APPENDIX B

g FACTORS FOR TENSION/COMPRESSION CYCLES

When a cyclic load goes through regions of compression there is no crack growth in these regions and the integration of Eq. [9] to obtain g should be taken only over the tensile portion of the cycle. In general, these integrals would have to be performed numerically.

One particular case of practical importance which can be integrated analytically is that of a sinusoidal stress wave with zero average stress. For the case of zero average stress, the time-to-failure ratio, Eq. [11], is rewritten in terms of the stress amplitude, σ_0 , as

$$t_c/t_s \approx g^{-1}(\sigma_s/\sigma_0)^n \quad [B1]$$

The g -factor is defined as

$$g = \frac{1}{\lambda} \int_0^\lambda [\sigma(t)/\sigma_0]^n dt, \quad [B2]$$

$[\sigma \geq 0]$

where $[\sigma \geq 0]$ means that regions of compression are omitted from the integral. For a sinusoidal stress wave

$$\sigma(t) = \sigma_0 \sin \omega t \quad [B3]$$

Eq. [B2] gives

$$g = \frac{1}{2\pi} \int_0^\pi \sin^n \theta d\theta$$

$$= \frac{1}{(4\pi)^{1/2}} \frac{\Gamma\left(\frac{n+1}{2}\right)}{\Gamma\left(\frac{n}{2}+1\right)}, \quad [\text{B4}]$$

where $\Gamma(x)$ is the gamma function. For larger n , Stirling's asymptotic series,

$$\Gamma(x+1) = (2\pi x)^{1/2} (x/e)^x \left[1 + \frac{1}{12x} + \frac{1}{288x^2} - \dots \right] \quad [\text{B5}]$$

can be used to give

$$g^{-1} \cong (2\pi n)^{1/2} \left[1 + \frac{1}{4n} + \frac{1}{32n^2} + \dots \right]. \quad [\text{B6}]$$

ACKNOWLEDGMENT

The authors wish to thank the Aeronautical Research Lab for supporting this work, under contract F 33615-73-M-6501

REFERENCES

1. C. S. Carter: *Corrosion*, 1971, vol. 27, pp. 471-77.
2. D. P. Williams and H. G. Nelson: *Met. Trans.*, 1972, vol. 3, pp. 2107-13.

3. W. G. Clark, Jr.: *J. of Engineering for Industry*, 1972, vol. 94, pp. 291-98.
4. R. P. Wei: *Eng. Frac. Mech.*, 1970, vol. 3, pp. 633-51.
5. H. H. Johnson and P. C. Paris: *Eng. Frac. Mech.*, 1968, vol. 1, pp. 3-45.
6. A. S. Tetelman: Acoustic Emission and Fracture Mechanics Testing of Metals and Composites, UCLA Report, UCLA-Eng-7249, July 1972.
7. S. M. El-Soudani and R. M. Pelloux: *Met. Trans.*, 1973, vol. 4, pp. 519-31.
8. S. M. Wiederhorn: *J. Amer. Ceram. Soc.*, 1967, vol. 50, pp. 407-14.
9. A. G. Evans: *J. Mater. Sci.*, 1972, vol. 7, pp. 1137-46.
10. D. A. Krohn and D. P. H. Hasselman: *J. Amer. Ceram. Soc.*, 1972, vol. 55, pp. 208-11.
11. L. S. Williams: *Mechanical Properties of Engineering Ceramics*, W. W. Krieger and H. Palmour, eds., Chap. 18, Interscience Publishers, New York, 1961.
12. C. Gurney and S. Pearson: *Proc. Roy. Soc.*, 1948, Series A, vol. 192, pp. 537-44.
13. A. G. Evans and S. M. Wiederhorn: NBS Report NBSIR 73-147, March 1973; *Intl. J. Frac. Mech.*, in press.
14. See for example, N. A. Weil and I. M. Daniel: *J. Amer. Ceram. Soc.*, 1964, vol. 47, pp. 268-74.
15. W. Weibull: *J. Appl. Mech.*, 1951, vol. 18, pp. 293-97.
16. D. P. Williams and A. G. Evans: *J. Testing and Evaluation*, 1973, vol. 1, pp. 264-70.
17. K. R. McKinney and H. L. Smith: *J. Amer. Ceram. Soc.*, 1973, vol. 56, pp. 30-32.
18. S. M. Wiederhorn, B. J. Hockey, and D. E. Roberts: *Phil. Mag.*, 1973, in press.
19. S. M. Wiederhorn, H. Johnson, A. M. Diness, and A. H. Heuer: *J. Amer. Ceram. Soc.*, 1974, in press.
20. See for example, J. C. Grosskreutz: *Fatigue—An Interdisciplinary Approach*, J. J. Burke, N. L. Reed, and V. Weiss, eds., pp. 27-59, Syracuse Univ. Press, Syracuse, New York, 1964.